

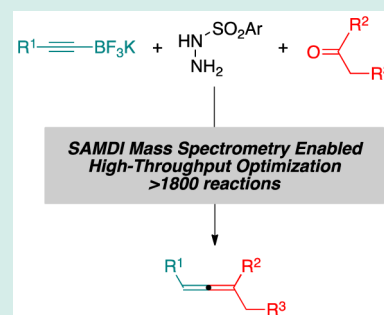
SAMDI Mass Spectrometry-Enabled High-Throughput Optimization of a Traceless Petasis Reaction

Abdallah B. Diagne, Shuheng Li, Gregory A. Perkowski, Milan Mrksich,* and Regan J. Thomson*

Department of Chemistry, Northwestern University, 2145 Sheridan Road, Evanston, Illinois 60208, United States

S Supporting Information

ABSTRACT: Development of the self-assembled monolayer/MALDI mass spectrometry (SAMDI) platform to enable a high-throughput optimization of a traceless Petasis reaction is described. More than 1800 unique reactions were conducted simultaneously on an array of self-assembled monolayers of alkanethiolates on gold to arrive at optimized conditions, which were then successfully transferred to the solution phase. The utility of this reaction was validated by the efficient synthesis of a variety of di- and trisubstituted allenes.



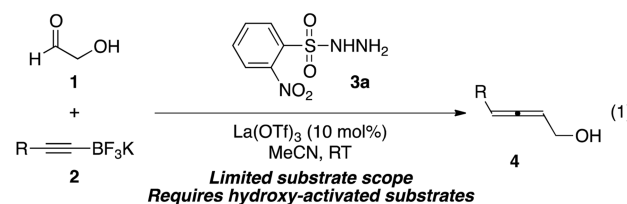
KEYWORDS: self-assembled monolayers, mass spectrometry, high-throughput experimentation, reaction optimization, allenes

The development of a synthetic methodology typically requires hundreds of reactions to be performed over a period of several months to identify effective combinations of reagents and to understand aspects of the structure–activity relationships. Several groups have reported progress with high-throughput approaches that significantly accelerate the development of reactions, yet this field is still in its early stages and requires further advances in methods that are efficient and applicable to a broad range of reaction types.¹ Here we describe the use of SAMDI mass spectrometry^{2–6} to quickly perform and evaluate hundreds of variants of a traceless Petasis reaction,⁷ and we identify structure–activity relationships that in turn guided the development of the corresponding solution-phase reaction.

In 2012, we reported the development of a novel method for synthesizing allenes that involved the direct coupling of α -hydroxy aldehydes (i.e., 1) with alkynyl trifluoroborate salts (i.e., 2) in the presence of 2-nitrobenzenesulfonylhydrazide (NBSH, 3a) and La(OTf)₃ (Figure 1, eq 1).⁷

While the reaction proceeded under mild reaction conditions to provide the desired allenes (i.e., 4) in good yield, attempts to expand the scope of the reaction to include substrates lacking α -hydroxyl substituents were unsuccessful. We viewed this shortcoming as an opportunity to explore the feasibility of conducting a high-throughput investigation of reaction parameters that would rapidly enable us to develop and optimize conditions to induce the desired transformation (Figure 1, eq 2). Ideally, the new reaction would proceed under mild reaction conditions, tolerate a range of aldehyde and ketone reaction partners (i.e., 5), and allow incorporation of a diverse set of substituents from the alkynyl trifluoroborate salt (i.e., 6), thereby affording access to a range of di- and

Previous work:



This work:

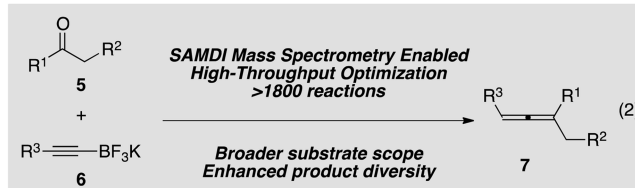


Figure 1. Traceless petasis reactions for the synthesis of allenes.

trisubstituted allene products (i.e., 7) complementary to other methods.⁸

A few recent reports show exciting progress toward reaction screening.^{9–20} For example, the groups of MacMillan⁹ and Hartwig,¹⁰ have reported gas chromatography–mass spectrometry methods for analyzing hundreds of reactions. Porco and co-workers reported an analogous high-throughput platform based on liquid chromatography mass spectrometry,¹¹ an approach subsequently improved upon in studies featuring ultra-performance liquid chromatography (UPLC)¹² and Merck's Multiple Injection in a Single Run (MISER) chromatography–mass spectrometry.^{13,14} Despite the limits

Received: August 21, 2015

Published: November 1, 2015

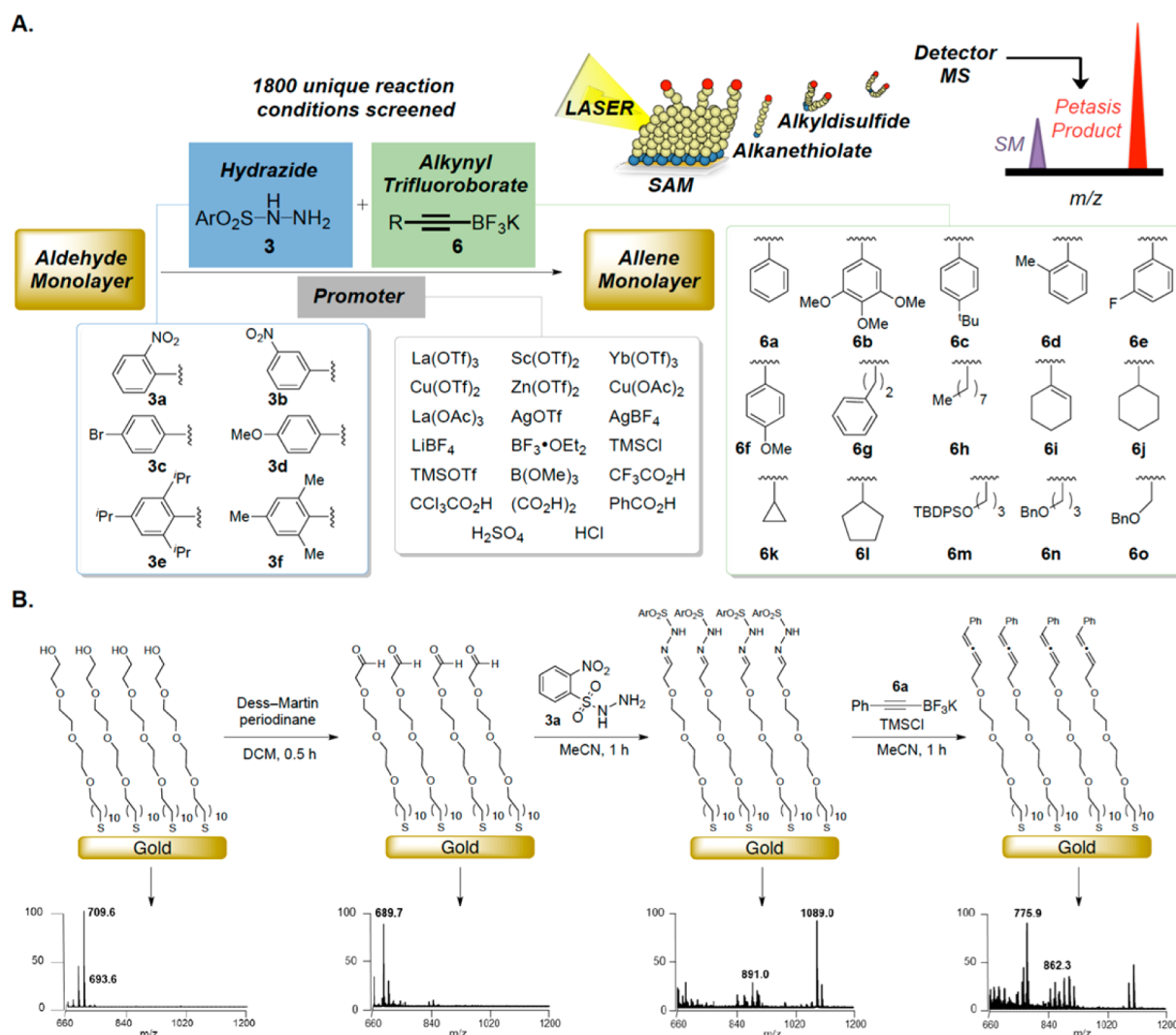


Figure 2. (A) Generalized workflow for the high-throughput SAMDI mass spectrometry-enabled investigation of the traceless Petasis reaction. (B) Representative example of generating surface-bound allenes by the initial oxidation of free alcohol-terminated monolayer to the corresponding aldehyde, followed by hydrazone formation and subsequent treatment with the appropriate alkynyl trifluoroborate salt and activator. Each step of the monolayer preparation could be monitored using mass spectrometry as shown.

on throughput imposed by the chromatographic step, these methods have high generality in identifying products of interest. Other methods use DNA microarray,¹⁵ immunoassay,¹⁶ and label-assisted mass spectrometry formats¹⁷ but require assay-specific substrates that can be difficult to develop or that may limit the scope of substrates or conditions to be screened. Other tag-free approaches based on infrared thermographic¹⁸ techniques overcome these limitations but lack generality. Efficient and general methods should avoid synthetic tagging and slow processing steps (i.e., chromatography), be compatible with high-throughput formats and allow for the rapid evaluation of reaction products and yields.

In this work, we demonstrate a reaction optimization using the SAMDI array-based mass spectrometry approach. In the SAMDI method, chemical or biochemical reactions are performed on functional groups presented on a self-assembled monolayer. The monolayers are then analyzed with matrix-assisted laser desorption-ionization (MALDI-ToF) mass spectrometry to identify the masses of reaction products.^{2–6} Hence, SAMDI provides a label-free analytical tool for the characterization of each individual reaction. A further benefit of

SAMDI is that reactions only need to be carried out on a picomolar scale, and the yields of these reactions can be quantitatively determined directly in a manner that obviates chromatographic purifications and synthetic labeling strategies. Here, we show how this method can be applied to determine optimal conditions that provide a high yield of the desired transformation in a single high-throughput experiment.

For the current study, we designed a high-throughput experiment that was based on 1800 unique combinations of 6 hydrazides **3a–f**, 15 alkynyl trifluoroborates **6a–o**, and 20 Lewis or Brønsted acid promoters (Figure 2A). These reactions were carried out on 6 arrays comprising steel plates having 384 gold spots each modified with a self-assembled monolayer of tri(ethylene glycol) terminated alkanethiolates. The carbonyl function required for the Petasis reaction was introduced on these gold islands by the direct Dess–Martin periodinane-mediated oxidation of the hydroxyl terminus (Figure 2B). We confirmed this transformation by analyzing the monolayers with SAMDI mass spectrometry, where the glycol-terminated monolayer showed peaks at m/z 693.6 and 709.6 (corresponding to the Na and K salts of the disulfide, respectively), and

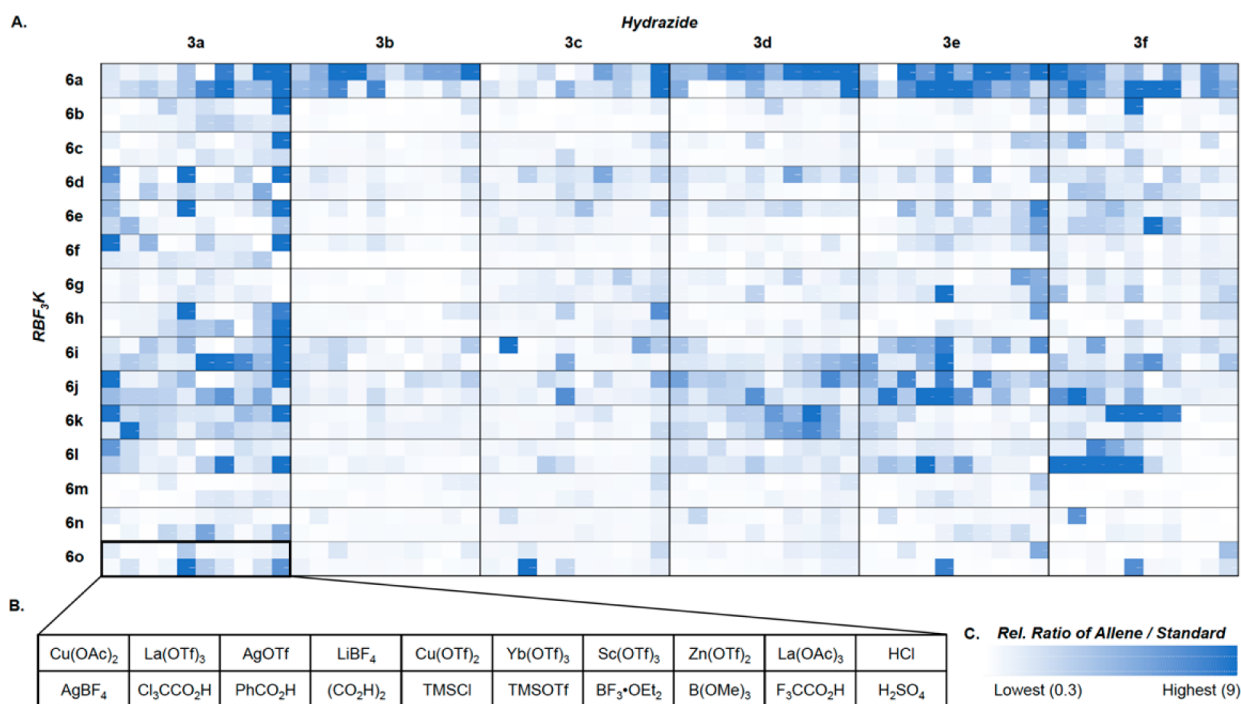


Figure 3. (A) Heat map showing 1800 unique reactions explored in the development and optimization of the traceless Petasis reaction. (B) Expanded inset showing the 2×10 matrix of Lewis and Brønsted acid promoters utilized for each combination of hydrazide and alkyne trifluoroborate. (C) Key to heat map that shows the efficiency of allene synthesis on the surface, as determined by the relative ratio of allene to internal standard according to SAMDI mass spectrometry. See the [Supporting Information](#) for further details.

where the oxidized monolayer showed a new peak at m/z 689.7 (Na salt of disulfide), as expected for generation of the aldehyde. The density of aldehyde functional groups was consistently more than 90% relative to the total alkanethiolates in the monolayer.

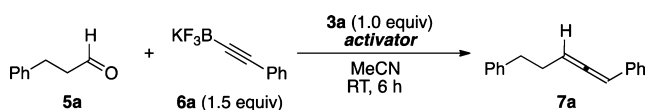
The next step in the workflow utilized automated liquid handling robots to deliver one unique arene-*N*-sulfonyl hydrazide **3a–f** (0.5 μ L of a 50 mM solution in acetonitrile) to 300 gold spots on each plate, leading to hydrazone formation after 1 h. [Figure 2B](#) shows a representative example using hydrazide **3a**, where the SAMDI spectrum shows the generation of the expected hydrazone peak at m/z 1089.0, as well as an analogous peak at m/z 891.0 that shows the mixed disulfide wherein one end contains the hydrazone and the second terminus remained an unfunctionalized hydroxyl group. The six disparate hydrazone-functionalized plates were then rinsed with acetone and the robot was further used to sequentially deliver each alkyne trifluoroborate **6a–o** (0.5 μ L of a 50 mM solution in acetonitrile) to 20 spots across 2 rows and 10 columns, and a unique Brønsted acid or Lewis acid promoter (0.5 μ L of a 50 mM solution in acetonitrile) to each spot. The reactions were allowed to proceed for another hour, and the plates were rinsed sequentially with water, acetone, and ethanol, followed by treatment with a THP matrix containing a known amount of an 11-amino acid peptide that served as an internal standard. The resulting allene-functionalized plates were also analyzed by SAMDI mass spectrometry. For the representative example in [Figure 2B](#), treatment of the NBSH (**3a**) derived hydrazone monolayer with trifluoroborate **6a** and chlorotrimethylsilane led to a new peak at m/z 775.9 corresponding to the allene product. Automated software was used to extract the intensities of the expected allene product of each reaction as well as of the internal standard, and their ratio was computed and visualized through conditional formatting in

a heat map for ease of analysis ([Figure 3](#), see the [Supporting Information](#) for complete experimental details).

An analysis of the heat map shown in [Figure 3](#) reveals that hydrazide **3a** (NBSH) proved to be the most efficient for forming allenes on the self-assembled monolayer, although the sterically congested, electron-rich hydrazides **3e** and **3f** were also reasonably effective. The phenylacetylene trifluoroborate **6a** generally provided the highest yields of the corresponding allene across the widest range of conditions, followed by the saturated and unsaturated cyclohexane derivatives **6i** and **6j**, and other aliphatic alkyne trifluoroborates **6h**, and **6k–l**. Other aryl substituted alkyne trifluoroborates **6b–f** showed attenuated reactivity, though they were effective in the presence of HCl as the promoter. Based on the consistently high-yielding surface reaction between alkyne trifluoroborate **6a** and hydrazide **3a**, we identified the six most efficient activators in the interfacial traceless Petasis reaction to be HCl, La(OAc)₃, Sc(OTf)₃, BF₃·OEt₂, TMSOTf, and TMSCl. We next evaluated these reagents in solution phase reactions using aliphatic aldehyde **5a** ([Table 1](#)).

We found a reasonable correlation between the reactivities on the surface and in solution, but also noted several differences. For example, the Lewis acids Sc(OTf)₃ and La(OAc)₃ gave low yields of the allene for the interfacial reactions ([Table 1](#), entries 2 and 4), unlike HCl and BF₃·OEt₂, each of which showed good reactivity on both the surface and the solution phase. TMSCl, in contrast, ([Table 1](#), entry 6) gave better yields in solution than did several activators that performed better in the surface reaction. These changes are similar to those observed when solvent effects are examined and are not unexpected, since solvation at the interfacial region is distinct from that in the bulk and presents a unique reaction environment.

Table 1. Comparison between Surface and Solution-Phase Reactions



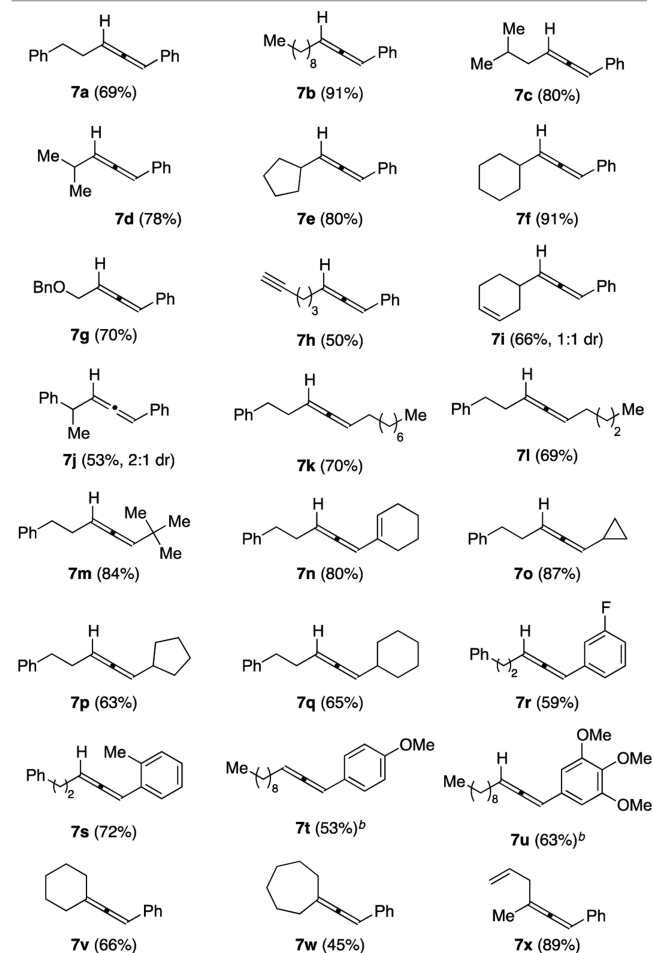
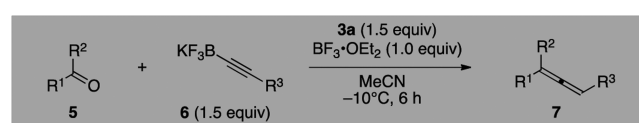
entry	activator	equiv	yield (%) ^a	surface rank ^b	solution rank ^c	Δ^d
1	HCl	1.0	46	1	2	-1
2	La(OAc) ₃	0.1 ^e	0	2	6	-4
3	BF ₃ ·OEt ₂	1.0	58	3	1	+2
4	Sc(OTf) ₃	0.1 ^e	10	4	5	-1
5	TMSOTf	1.0	20	5	4	+1
6	TMSCl	1.0	35	6	3	+3

^aIsolated yield of **7a** using 0.5 mmol of **5a**. ^bDetermined by the average yield of Petasis reactions of **6a**, **6i**, and **6j** with **3a** relative to an internal standard. ^cBased on isolated yield of **14**. ^d $\Delta = [\text{surface ranking}] - [\text{solution ranking}]$. ^eUse of stoichiometric quantities gave 0% yield of allene **7a**.

Ultimately, we found that BF₃·OEt₂ was the most effective activator for the solution reaction, providing the product in 58% yield using 1.5 equiv of alkyne **6a** and 1.0 equiv of NBSH (**3a**). A related reaction involving the addition of lithiated acetylides into preformed *N*-aziridinylimines has been reported previously by Kim and co-workers, although only 12 examples were given and the reaction required 3.0 equiv of the alkyne reagent to generate good yields.²¹ We therefore chose to further explore the efficiency of the BF₃·OEt₂ promoted reaction in solution (Table 2) to devise a more general and widely applicable method for allene synthesis. The initial “hit” of 58% yield for the synthesis of allene **7a** was readily increased to 69% yield when the amount of NBSH (**3a**) used was increased from 1.0 equiv to 1.5 equiv, and the temperature was lowered from room temperature to -10 °C. Attempts to decrease the amount of alkyne **6a** or BF₃·OEt₂ used in the reaction led to diminished yields of the allene **7a**, while increasing the amount of **6a** beyond 1.5 equiv had no effect. Thus, the high-throughput investigation enabled by SAMDI, conducted on significantly miniaturized scales, allowed for the rapid discovery of effective reaction conditions, thereby significantly reducing the necessary amount of solution-phase optimization to only a few focused reactions.

Under the newly devised conditions, a number of allenes could be accessed from a variety of cyclic and acyclic aliphatic aldehydes and ketones (Table 2).

A range of linear, branched and cyclic aldehydes delivered disubstituted allenes in good to excellent yield upon reaction with phenylacetylene trifluoroborate **6a** (Table 2, **7a–7f**). Benzyl ether, alkene and alkyne functionalized aldehydes proved to be tolerant of the reaction conditions (Table 2, **7g–7i**), with the formation of allene **7h** demonstrating that terminal alkynes do not participate in the reaction (Table 2, **7h**). For aldehydes possessing α -stereocenters, the reaction proved to be poorly diastereoselective (Table 2, **7i** and **7j**). The alkynyl trifluoroborate partner could also be readily changed, allowing access to a diverse set of aryl and alkyl substituted products (Table 2, **7k–7u**). The oxygenated derivatives **7t** and **7u** were accessed in reasonable yields when the reactions were conducted at lower concentrations. The parent alkynyl trifluoroborates for these substrates showed reduced solubility in acetonitrile, and an increased propensity toward unproductive protodeboronation under the standard reaction conditions.

Table 2. Scope of the Solution Phase Traceless Petasis Allene Synthesis^a

^aIsolated yields from reactions conducted using 0.5 mmol of **5**, 0.75 mmol of **6**, and 0.75 mmol of **3a** in MeCN (2 mL). ^bReaction conducted using 5 mL of MeCN.

Finally, we demonstrated that the traceless allene synthesis is also tolerant of both cyclic and acyclic ketones as reaction partners, allowing the generation of trisubstituted allenes in modest to high yields (Table 2, **7v–7x**). The relatively mild reaction conditions, low reaction temperature and operational simplicity of this allene synthesis are particularly noteworthy, especially in the context of trisubstituted allenes, as many of the previously established methods require relatively harsh conditions and elevated temperatures.^{22–24}

In summary, we have demonstrated the application of SAMDI mass spectrometry for the high-throughput development and optimization of organic reaction parameters. By using the automated ability of the SAMDI mass spectrometry platform to rapidly conduct and analyze sequential reactions at miniaturized scale, we were able to prepare and analyze 1800 unique variations of a traceless Petasis reaction in order to provide initial reaction conditions and early insight into substrate scope. Translation of the most efficient surface-based conditions to the solution phase rapidly established an optimal set of reaction conditions to allow for preparative scale

reactions to be run with minimal additional optimization necessary. Ultimately, an operationally simple and high yielding allene synthesis was established that displays a significantly broadened substrate scope in comparison to the originally devised traceless Petasis coupling,³ as it obviates the presence of a hydroxyl activating group. The results of the study delineated herein also set the stage for the further development and refinement of SAMDI mass spectrometry-based methods for future application to other organic reactions.

■ ASSOCIATED CONTENT

● Supporting Information

The Supporting Information is available free of charge on the ACS Publications website at DOI: 10.1021/acscombsci.5b00131.

Complete details of the high-throughput SAMDI mass spectrometry setup, all experimental procedures, and complete characterization for all new compounds (IR, MS, NMR) (PDF)

■ AUTHOR INFORMATION

Corresponding Authors

*E-mail: milan.mrksich@northwestern.edu.

*E-mail: r-thomson@northwestern.edu.

Author Contributions

The manuscript was written through contributions of all authors. All authors have given approval to the final version of the manuscript. A.B.D. and S.L. contributed equally.

Notes

The authors declare no competing financial interest.

■ ACKNOWLEDGMENTS

We gratefully acknowledge financial support from Northwestern University, and the National Science Foundation (CHE1361173 to R.J.T.). A.B.D. thanks the ARCS Foundation for the Daniel F. and Ada L. Rice Foundation Scholarship.

■ REFERENCES

- (1) Collins, K. D.; Gensch, T.; Glorius, F. Contemporary Screening Approaches to Reaction Discovery and Development. *Nat. Chem.* **2014**, *6*, 859–871.
- (2) Su, J.; Mrksich, M. Using Mass Spectrometry to Characterize Self-Assembled Monolayers Presenting Peptides, Proteins, and Carbohydrates. *Angew. Chem., Int. Ed.* **2002**, *41*, 4715–4718.
- (3) Su, J.; Mrksich, M. Using Maldi-Tof Mass Spectrometry to Characterize Interfacial Reactions on Self-Assembled Monolayers. *Langmuir* **2003**, *19*, 4867–4870.
- (4) Li, J.; Thiara, P. S.; Mrksich, M. Rapid Evaluation and Screening of Interfacial Reactions on Self-Assembled Monolayers. *Langmuir* **2007**, *23*, 11826–11835.
- (5) Gurard-Levin, Z. A.; Scholle, M. D.; Eisenberg, A. H.; Mrksich, M. High-Throughput Screening of Small Molecule Libraries Using Samdi Mass Spectrometry. *ACS Comb. Sci.* **2011**, *13*, 347–350.
- (6) Montavon, T. J.; Li, J.; Cabrera-Pardo, J. R.; Mrksich, M.; Kozmin, S. A. Three-Component Reaction Discovery Enabled by Mass Spectrometry of Self-Assembled Monolayers. *Nat. Chem.* **2012**, *4*, 45–51.
- (7) Mundal, D. A.; Lutz, K. E.; Thomson, R. J. A Direct Synthesis of Allenes by a Traceless Petasis Reaction. *J. Am. Chem. Soc.* **2012**, *134*, 5782–5785.
- (8) Yu, S.; Ma, S. How Easy Are the Syntheses of Allenes? *Chem. Commun.* **2011**, *47*, 5384–5418.
- (9) McNally, A.; Prier, C. K.; MacMillan, D. W. C. Discovery of an α -Amino C–H Arylation Reaction Using the Strategy of Accelerated Serendipity. *Science* **2011**, *334*, 1114–1117.
- (10) Robbins, D. W.; Hartwig, J. F. A Simple, Multidimensional Approach to High-Throughput Discovery of Catalytic Reactions. *Science* **2011**, *333*, 1423–1427.
- (11) Beeler, A. B.; Su, S.; Singleton, C. A.; Porco, J. A. Discovery of Chemical Reactions through Multidimensional Screening. *J. Am. Chem. Soc.* **2007**, *129*, 1413–1419.
- (12) DiRocco, D. A.; Dykstra, K.; Krska, S.; Vachal, P.; Conway, D. V.; Tudge, M. Late-Stage Functionalization of Biologically Active Heterocycles through Photoredox Catalysis. *Angew. Chem., Int. Ed.* **2014**, *53*, 4802–4806.
- (13) Bellomo, A.; Celebi-Olcum, N.; Bu, X.; Rivera, N.; Ruck, R. T.; Welch, C. J.; Houk, K. N.; Dreher, S. D. Rapid Catalyst Identification for the Synthesis of the Pyrimidinone Core of HIV Integrase Inhibitors. *Angew. Chem., Int. Ed.* **2012**, *51*, 6912–6915.
- (14) Buitrago Santanilla, A.; Regalado, E. L.; Pereira, T.; Shevlin, M.; Bateman, K.; Campeau, L.-C.; Schneeweis, J.; Berritt, S.; Shi, Z.-C.; Nantermet, P.; Liu, Y.; Helmy, R.; Welch, C. J.; Vachal, P.; Davies, I. W.; Cernak, T.; Dreher, S. D. Nanomole-Scale High-Throughput Chemistry for the Synthesis of Complex Molecules. *Science* **2015**, *347*, 49–53.
- (15) Chen, Y.; Kamlet, A. S.; Steinman, J. B.; Liu, D. R.; Biomolecule-Compatible Visible-Light-Induced, A. Azide Reduction from a DNA-Encoded Reaction-Discovery System. *Nat. Chem.* **2011**, *3*, 146–153.
- (16) Kolodych, S.; Rasolofonjatovo, E.; Chaumontet, M.; Nevers, M.-C.; Créminon, C.; Taran, F. Discovery of Chemoselective and Biocompatible Reactions Using a High-Throughput Immunoassay Screening. *Angew. Chem., Int. Ed.* **2013**, *52*, 12056–12060.
- (17) Cabrera-Pardo, J. R.; Chai, D. I.; Liu, S.; Mrksich, M.; Kozmin, S. A. Label-Assisted Mass Spectrometry for the Acceleration of Reaction Discovery and Optimization. *Nat. Chem.* **2013**, *5*, 423–427.
- (18) Cypes, S.; Hagemeyer, A.; Hogan, Z.; Lesik, A.; Streukens, G.; Volpe, A. F., Jr.; Weinberg, W. H.; Yaccato, K. High Throughput Screening of Low Temperature Co Oxidation Catalysts Using Ir Thermography. *Comb. Chem. High Throughput Screening* **2007**, *10*, 25–35.
- (19) Preshlock, S. M.; Ghaffari, B.; Maligres, P. E.; Krska, S. W.; Maleczka, R. E.; Smith, M. R. High-Throughput Optimization of Ir-Catalyzed C–H Borylation: A Tutorial for Practical Applications. *J. Am. Chem. Soc.* **2013**, *135*, 7572–7582.
- (20) Friedfeld, M. R.; Shevlin, M.; Hoyt, J. M.; Krska, S. W.; Tudge, M. T.; Chirik, P. J. Cobalt Precursors for High-Throughput Discovery of Base Metal Asymmetric Alkene Hydrogenation Catalysts. *Science* **2013**, *342*, 1076–1080.
- (21) Kim, S.; Cho, C. M.; Yoon, J.-Y. Reaction of N-Aziridinylimines with Alkynylborane Reagents. A New Route to Allenes from Aldehydes and Ketones. *J. Org. Chem.* **1996**, *61*, 6018–6020.
- (22) Xiao, Q.; Xia, Y.; Li, H.; Zhang, Y.; Wang, J. Coupling of N-Tosylhydrazones with Terminal Alkynes Catalyzed by Copper(I): Synthesis of Trisubstituted Allenes. *Angew. Chem., Int. Ed.* **2011**, *50*, 1114–1117.
- (23) Tang, X.; Zhu, C.; Cao, T.; Kuang, J.; Lin, W.; Ni, S.; Zhang, J.; Ma, S. Cadmium Iodide-Mediated Allenylation of Terminal Alkynes with Ketones. *Nat. Commun.* **2013**, *4*, 2450.
- (24) Tang, X.; Han, Y.; Ma, S. Cadmium Iodide Mediated Allenylation of Terminal Alkynes for the Synthesis of Methyl-Substituted Allenes. *Org. Lett.* **2015**, *17*, 1176–1179.